

Rats with a Human Mutation of NFU1 Develop Pulmonary Hypertension

Maki Niihori^{1*}, Cody A. Eccles^{1*}, Sergey Kurdyukov¹, Marina Zemskova¹, Mathews Valuparampil Varghese¹, Anna A. Stepanova², Alexander Galkin², Ruslan Rafikov¹, and Olga Rafikova¹

¹Division of Endocrinology, Department of Medicine, University of Arizona College of Medicine, Tucson, Arizona; and ²Division of Neonatology, Department of Pediatrics, Columbia University, New York, New York

ORCID ID: 0000-0001-5950-4076 (R.R.).

Abstract

NFU1 is a mitochondrial protein that is involved in the biosynthesis of iron-sulfur clusters, and its genetic modification is associated with disorders of mitochondrial energy metabolism. Patients with autosomal-recessive inheritance of the NFU1 mutation G208C have reduced activity of the respiratory chain Complex II and decreased levels of lipoic-acid-dependent enzymes, and develop pulmonary arterial hypertension (PAH) in ~70% of cases. We investigated whether rats with a human mutation in NFU1 are also predisposed to PAH development. A point mutation in rat NFU1^{G206C} (human G208C) was introduced through CRISPR/Cas9 genome editing. Hemodynamic data, tissue samples, and fresh mitochondria were collected and analyzed. NFU1^{G206C} rats showed increased right ventricular pressure, right ventricular hypertrophy, and high levels of pulmonary artery remodeling. Computed tomography and angiography of the pulmonary vasculature indicated severe angioobliterative changes in NFU1^{G206C} rats. Importantly, the penetrance of the PAH phenotype was found to be more prevalent in females than in males, replicating the established sex difference among patients with PAH. Male and female homozygote rats exhibited decreased expression and activity of mitochondrial Complex II, and markedly decreased pyruvate dehydrogenase activity and lipoate binding. The limited development of PAH in males correlated with the preserved levels of oligomeric NFU1, increased expression of ISCU (an alternative branch of the iron-sulfur assembly system), and

increased complex IV activity. Thus, the male sex has additional plasticity to overcome the iron-sulfur cluster deficiency. Our work describes a novel, humanized rat model of NFU1 deficiency that showed mitochondrial dysfunction similar to that observed in patients and developed PAH with the same sex dimorphism.

Keywords: pulmonary arterial hypertension; iron-sulfur cluster; mitochondrial dysfunction; Complex II; sex difference

Clinical Relevance

This study describes the first humanized genetic rat model to spontaneously develop pulmonary arterial hypertension (PAH). This model was achieved by a CRISPR/Cas9 gene modification that introduced a 1-nt point mutation into the iron-sulfur cluster scaffold protein NFU1. This resulted in whole-body expression of mutant NFU1 G208C, which is identical to the clinically relevant mutation in patients that results in multiple mitochondrial dysfunctions syndrome 1 and manifestation of PAH. Rats with deficient NFU1 produced a strong PAH phenotype with proliferative changes in the lung vasculature and right-heart hypertrophy. We also provide a molecular characterization of the model.

(Received in original form February 25, 2019; accepted in final form August 27, 2019)

*These authors contributed equally to this work.

Supported by National Institutes of Health grants R01HL133085 (O.R.) and R01HL132918 (R.R.).

Author Contributions: Conception and design: R.R. and O.R. Analysis and interpretation: M.N., C.A.E., S.K., M.Z., M.V.V., and A.A.S. Drafting of the manuscript for important intellectual content: A.G., R.R., and O.R.

Correspondence and requests for reprints should be addressed to Ruslan Rafikov, Ph.D., Division of Endocrinology, Department of Medicine, University of Arizona College of Medicine, Room 4220, 1501 N. Campbell Avenue, Tucson, AZ 85721. E-mail: ruslanrafikov@deptofmed.arizona.edu.

This article has a related editorial.

This article has a data supplement, which is accessible from this issue's table of contents at www.atsjournals.org.

Am J Respir Cell Mol Biol Vol 62, Iss 2, pp 231–242, Feb 2020

Copyright © 2020 by the American Thoracic Society

Originally Published in Press as DOI: 10.1165/rcmb.2019-0065OC on August 28, 2019

Internet address: www.atsjournals.org

Mitochondrial dysfunction was previously reported in animal models and patients with pulmonary arterial hypertension (PAH) (1–6). The glycolytic switch, when vascular cells shift from oxidative phosphorylation (OXPHOS) to glycolysis for energy production in the lungs, is well established in PAH (1, 7–9). “Mitochondrial dysfunction” is a broad term for multiple issues that affect the normal function of the organelle, including inhibited OXPHOS (1), decreased pyruvate dehydrogenase (PDH) complex activity (10), decreased fatty acid transport and oxidation (11, 12), increased mitochondria-derived reactive oxygen species production (13, 14), and increased mitochondrial fission (6, 15). Our previous study also showed that cells isolated from animals with pulmonary hypertension (PH) showed decreased activity of Complexes I, II, and III (1). Inhibition of Complex III by Antimycin A in healthy rats resulted in a glycolytic switch in the lungs and led to increased pulmonary pressure 24 days after the Antimycin A injection (16). Therefore, the compromised function of mitochondrial respiratory complexes can induce PAH. Our goal in the present study was to find a genetic way to induce the OXPHOS dysfunction and to demonstrate that this dysfunction is sufficient to induce PH.

Mutations in the iron-sulfur (Fe-S) cluster regulatory proteins often result in mitochondrial disease in humans (17–21). Fe-S clusters are important cofactors in Complexes I, II, and III, which are responsible for electron transfer. Without properly assembled Fe-S clusters, the respiratory chain becomes dysfunctional. In humans with genetic mutations in the *ISCU*, *NFU1*, and *BOLA3* genes, which are responsible for Fe-S cluster biogenesis and their insertion into respiratory complexes, respiratory chain dysfunction produces myopathy, exercise intolerance, and sometimes lethal conditions (21–24). Interestingly, patients with a genetic mutation in Fe-S clusters develop PAH at a much higher rate than the general population (20, 24, 25). A 1-nt mutation in *NFU1* that leads to Gly208Cys replacement produces multiple mitochondrial dysfunctions syndrome 1 (MMDS1) in patients (25). MMDS1 leads to encephalopathy and is characterized by decreased Complex I and II activities, lipoic acid synthase (LAS) deficiency, and PH in 70% of cases, whereas in humans the incidence rate of PAH is 10–50 cases per

million (or 0.001–0.005%). In this work, we reproduced the same human mutation in normotensive Sprague Dawley (SD) rats using the CRISPR/Cas9 editing technique to determine whether Fe-S cluster deficiency can induce PH in rats.

Methods

NFU1 Point Mutation Rats and Genotyping

The SD rat model with a point mutation (G206C, GGC–TGC) at the rat *Nfu1* locus, engineered by CRISPR/Cas9-mediated genome editing, was created by Cyagen Biosciences Inc. The rat *Nfu1* gene is located at rat chromosome 4, and G206C is located on exon 7 out of eight exons identified. The G206C in donor oligo was introduced into exon 7 by homology-directed repair. Cas9 mRNA, single-guide RNA, and donor oligo were coinjected into zygotes. We obtained three heterozygote mutant (HZ) males (NFU1G206C/+) and three HZ females (NFU1G206C/+), and they became founders of the colony. The pups were genotyped by PCR with the following primers: CCTGCTGCTAACCTGAGTTCCAT (forward) and TTGTACTGTGACA CCCAGCCTGT (reverse, fluorescently labeled with 6-fluorescein amidite [FAM]). Digestion of PCR products by the *BsrI* restriction enzyme gave two products: 141 bp (homozygous mutant) and 447 bp (wild-type [WT]). *Nfu1* point mutation rats were bred in-house and the colony was kept in a University Animal Care facility at the University of Arizona. The animals were kept in a 12-hour light/dark cycle and received standard rodent food and water *ad libitum*. The SD male and female age-matched rats were purchased from Charles River. All experimental procedures were approved by the University of Arizona’s Institutional Animal Care and Use Committee.

Hemodynamic Measurements and Organ Harvest

The animals were analyzed at the age of 10–12 weeks. The animals were anesthetized (Inactin, T133, 100 mg/kg i.p.; Sigma-Aldrich) and instrumented for the measurement of right ventricle (RV) hemodynamics as previously described (26). A customized pressure transducer catheter (SPR-513; Millar Instruments) connected to

a Millar Transducer Control Unit TC-510 and a PL3504 PowerLab 4/35 data acquisition system (ADInstruments) was inserted into the RV via the right jugular vein and right atrium. For systemic blood pressure measurements, another pressure transducer catheter (SPR 671; Millar Instruments) was inserted into the right carotid artery. A 15- to 30-minute stabilization period was permitted before a 30-minute recording of RV pressure was obtained, as previously described (26, 27). Briefly, a PE-240 polyethylene tube was inserted into the trachea to facilitate breathing. At the end of the pressure recording, the trachea catheter was connected to a Harvard Rodent Ventilator (model 683; Harvard Apparatus), the thorax was opened, the left atrium was cut, and the lungs were flushed with saline (0.9% sodium chloride) via a needle inserted into the RV. The animals were then killed by removing the heart/lung block. The lungs, RV, and left ventricle + septum (LV+S) were dissected and weighed. RV function was analyzed using the Blood Pressure Software module (AD Instruments).

Statistical Analysis

Statistical calculations were performed using GraphPad Prism software, version 7.04. The mean value (\pm SEM) was calculated for all samples, and significance was determined by either the unpaired *t* test or ANOVA. For ANOVA, Newman-Keuls or Bonferroni multiple-comparison tests were used to compare the selected pairs of columns. A *P* value of <0.05 was considered significant. The Grubbs test (extreme Studentized deviate) was used to determine the significant outliers. This criterion was predetermined before initiation of the data analysis.

For details regarding all other methods used in this work, please refer to the data supplement.

Results

PH Phenotype

In this study, we used WT rats and rats heterozygous (HZ) and homozygous (HM) for the *NFU1*^{G206C} mutation (human G208C). Because PAH has a sex specificity, we also separated the rats by sex. Our hemodynamic data indicated a trend in RV systolic pressure (RVSP), with an increase in HZ females and a significant increase in HM females (Figure 1A). This elevation of

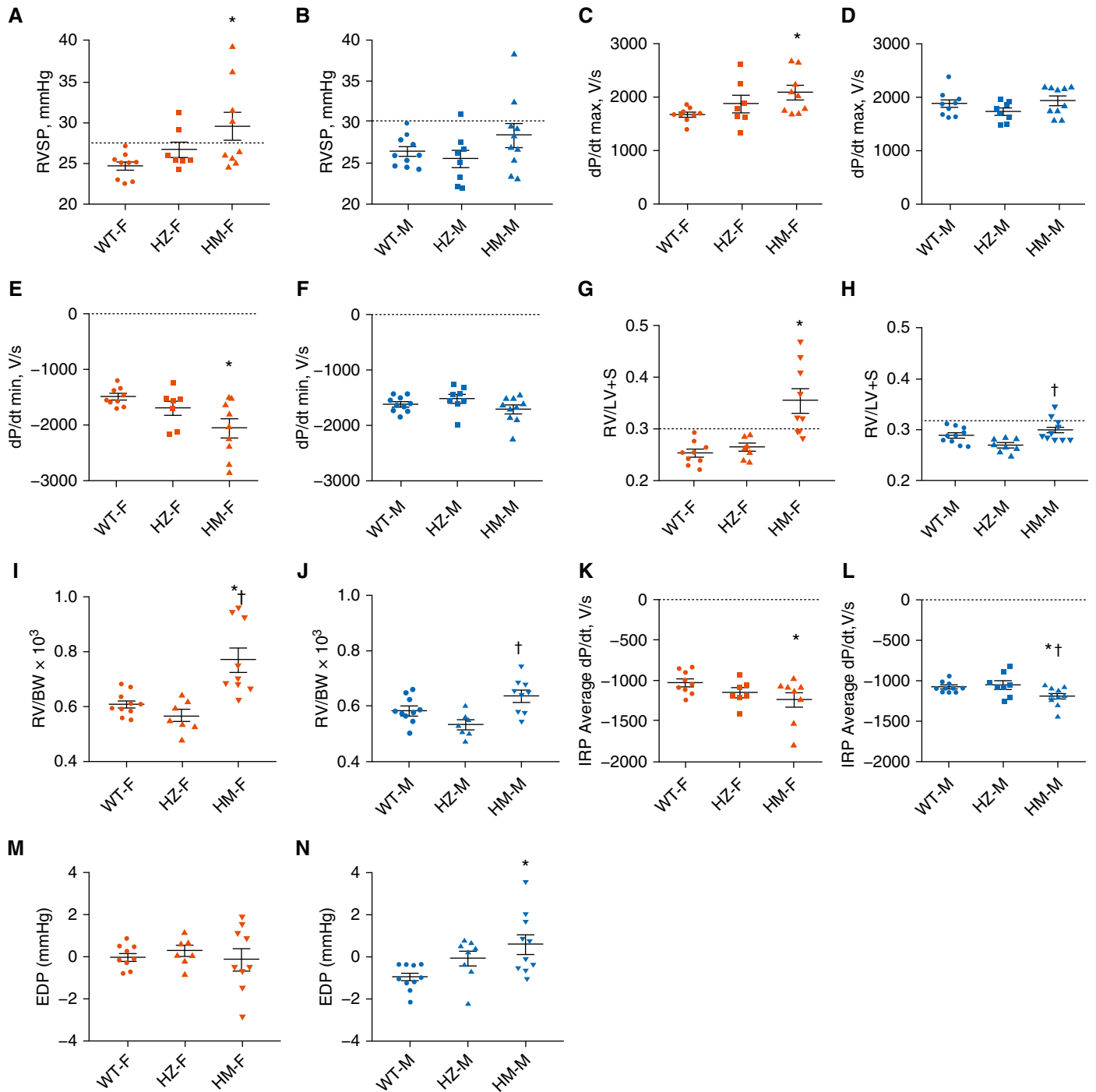


Figure 1. Hemodynamic changes in NFU1 mutant rats. (A) Right ventricular systolic pressure (RVSP) was slightly increased in heterozygote female rats (HZ-F) and significantly elevated in homozygote female rats (HM-F). (B) RVSP was only slightly elevated in HM males (HM-M). (C–F) RV dP/dt max (C) as a measure of RV contractility and RV dP/dt min (E) as a measure of RV contractility was significantly elevated in HM-F, but not HM-M, rats (D and F). (G) The Fulton index, the ratio of the RV to the left ventricle plus septum (RV/[LV+S]), was insignificantly increased in HZ-F and markedly increased in HM-F. (H) In males, the Fulton index was significantly higher in the HM group than in the HZ group. (I and J) The RV weight to body weight ratio (RV/BW) showed a trend similar to that observed for the Fulton index in females and males. (K and L) The average dP/dt during the isovolumetric relaxation period (IRP) as a measure of RV diastolic relaxation was significantly decreased in the HM rats of either sex. (M and N) Although the end-diastolic pressure (EDP) showed no changes in females (M), it was found to be significantly elevated in the HM-M group (N), confirming a more pronounced RV diastolic dysfunction in males. Data are presented as mean \pm SEM, $n = 7$ –10, * $P < 0.05$ versus WT, ANOVA. † $P < 0.05$ versus HZ. dP/dt = a mathematical expression meaning derivative of pressure over time; F = female; M = male; WT = wild type.

RVSP is similar to that observed in monocrotaline (MCT) and hypoxia rodent models, but is relatively mild in comparison with the Sugden/hypoxia model. Interestingly, males did not show an increase in RVSP in either HZ or HM rats, except for two HM rats whose pressure increased above the normal range (Figure 1B). This is a significant observation that one point mutation in the NFU1 protein can lead to a sex dimorphism similar to clinical observations in patients with PAH. The changes in RVSP corresponded to changes in RV dp/dt max and RV dp/dt min, the measures of RV contractility and relaxation (Figures 1C–1F). Thus, only female rats showed a significant increase in both parameters (Figures 1C and 1F), supporting the finding that the female group had an elevated RV workload. The Fulton index, a measure of RV hypertrophy, was elevated in HZ and significantly increased in HM females (Figure 1G). Importantly, RV hypertrophy was more pronounced than the increased RVSP in the female HM group. In males, we observed a significant but mild increase in RV hypertrophy between the HM and HZ groups (Figure 1H). To confirm that the increase in RV weight was not due to changes in the LV size, we also calculated the RV weight to body weight ratio, and it showed a trend similar to that observed for the Fulton index (Figures 1I and 1J). To evaluate the potential outcomes of RV hypertrophy discovered in HM rats, we investigated the RV diastolic function, a major determinant of ventricular performance (28). The average rate of pressure change during the isovolumic relaxation period (IRP ave dp/dt) was found to be significantly reduced in both sexes (Figures 1K and 1L). These changes pointed to an impairment of RV relaxation that seems to be independent of the RV

load or RV remodeling. Moreover, the male group that had only a mild increase in RVSP and RV remodeling showed a significantly elevated end-diastolic pressure (Figure 1N). Thus, despite the lower susceptibility of males to PH, our model reproduces the well-established predisposition of the male sex to develop RV dysfunction (27, 29). Notably, the animals from all experimental groups had comparable heart rates, confirming the equal level of anesthesia in each group (Table 1). Although the mean arterial pressure was found to be slightly decreased in both sexes, the absence of hypertensive responses in the systemic circulation highlights the specific sensitivity of the pulmonary vasculature to mitochondrial dysfunction induced by the NFU1 mutation. We also confirmed the absence of hypertrophic changes in the LV (Table 1).

Histological assessments of the lungs indicated a significantly increased vascular occlusive score, confirming a severe vascular remodeling in the pulmonary arteries of NFU1 mutant rats of both sexes (Figures 2A and 2B). Moreover, a three-dimensional analysis (Figure 2C) of the pulmonary vasculature and microangiography of the small pulmonary arteries (Figure 2D) revealed strong changes in the pulmonary vasculature morphology of the NFU1 mutant rats. Both analyses showed a significant vasoocclusive disease of the medium and small pulmonary arteries, confirming the development of the PH phenotype in rats with the NFU1 mutation.

Respiratory System Abnormalities

The mutation of NFU1^{G206C} in humans results in a deficiency of Complexes I and II due to a decreased ability of NFU1 to insert Fe-S clusters. To determine whether the rat

NFU1^{G206C} model recapitulates similar changes in respiratory complex activities, we examined freshly isolated mitochondria. Our data indicated a significant decrease in Complex I activity in HM females (Figures 3A and 3B). In HM males, although Complex I activity was decreased, this effect did not reach significance (Figure 3D). Complex II activity was found to be inhibited in the HM group of both sexes (Figure 3E). Interestingly, complex IV activity did not change in females but was significantly elevated in HM males (Figures 3C and 3F). Thus, the male group could have a compensatory mechanism for overcoming a Complex II deficiency, which could be responsible for the weak PH phenotype in HM males. We also assessed the expression levels of each complex. In accordance with our activity data, both Complex I (NDUF8b) and Complex II (SDHA and SDHB) subunits were markedly downregulated in HM females (Figures 4A–4D). Levels of Complexes III, IV, and V in the HZ and HM groups were similar to WT levels (Figures 4E–4G). In males, the Complex I subunit showed reduced expression in the HM group (Figures 4H and 4I). SDHA (one of the two Complex II subunits) was decreased (Figures 4J and 4K). Male rats also demonstrated increased Complex III expression levels in HZ and HM males (Figure 4L), whereas Complexes IV and V were unchanged (Figures 4M and 4N). Taken together, these observations show the severe effect of the NFU1^{G206C} mutation on Fe-S-containing Complexes I and II in both males and females; however, in HM males, Complex III was upregulated and Complex IV activity was increased. This may reflect an additional compensation in males in response to the decreased electron flow from the first two complexes. The upregulation of the

Table 1. Body Weight, Heart Rate, Systemic Pressure, and Left-Heart Parameters

	Female			Male		
	WT	HZ	HM	WT	HZ	HM
BW, g	235.5 ± 12.3	323.7 ± 28.3*	228.4 ± 28.2	415.9 ± 21.3	441.9 ± 80.1*	369.8 ± 60.5*
HR, BPM	357.6 ± 38.2	387.6 ± 52.0	386.1 ± 38.3	348.6 ± 13.6	361.6 ± 28.7	371.9 ± 27.1
MAP, mm Hg	102.6 ± 16.4	NA	83.8 ± 5.6*	105.0 ± 9.1	NA	88.7 ± 1.8*
LV/BW × 10 ³	2.47 ± 0.20	2.15 ± 0.12*	2.19 ± 0.16*	2.04 ± 0.17	2.00 ± 0.10	2.12 ± 0.18

Definition of abbreviations: BPM = beats per minute; BW = body weight; HM = homozygote; HR = heart rate; HZ = heterozygote; LV/BW = left ventricle weight to body weight ratio; MAP = mean arterial pressure; NA = not available; WT = wild type.

**P* < 0.05 compared with the WT.

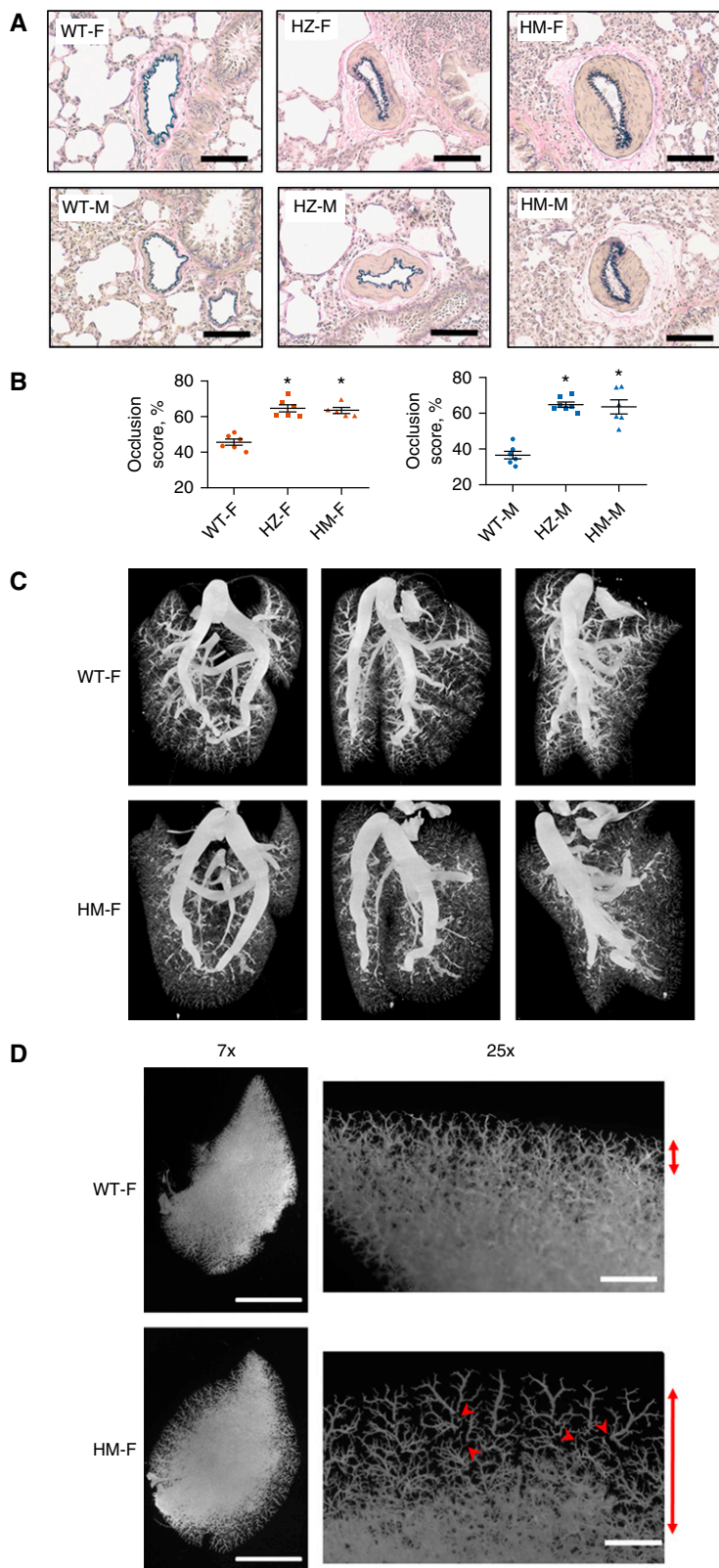


Figure 2. (A) Histological changes in the lungs. Representative images of Verhoeff–van Gieson-stained lungs show a severe remodeling of pulmonary arteries. Scale bars: 100 μ m. (B) Quantitative analysis of pulmonary artery remodeling. The vascular occlusion score was significantly increased in both male and female HZ and HM groups compared with control (mean \pm SEM, $n=5-7$, $*P < 0.05$

respiratory chain at Complexes III and IV may be involved in the observed sex dimorphism in the PAH phenotype.

NFU1 Oligomerization

It was previously reported that NFU1 requires the dimerization step to bind Fe-S clusters, and furthermore, that dimers can assemble hexamers to form an active holoenzyme (30). Using lung lysates, we tested whether the oligomerization of NFU1 is compromised by mutation. Our data indicated significantly increased hexamers in the HZ female group and reduced hexamers in the HM female group (Figures 5A and 5B). The dimerization of NFU1 was not altered in females (Figure 5C). In contrast, in males, hexamers were preserved (Figures 5D and 5E); however, dimers were significantly reduced in the HM group (Figure 5F). The preservation of hexamers could also contribute to the ability of NFU1-deficient male rats to resist the development of PAH. It is important to note that the total content of NFU1 protein was not affected by the mutation.

PDH Activity

LAS is an important Fe-S cluster-containing protein that is dependent on NFU1 and has been shown to be inhibited in patients with the NFU1^{G208C} mutation. Reduced production of lipoic acid, the cofactor of the PDH complex, hinders the formation of acetyl coenzyme A from pyruvate, affecting the tricarboxylic acid (TCA) cycle and OXPHOS. Inhibited PDH activity has also been linked to the development of PH (31). Thus, we sought to determine whether the expression and activity of PDH were affected in NFU1-deficient rats. Our data indicate that females in the HM group had increased protein levels of PDH (Figures 6A and 6B). However, the activity of PDH was inhibited (Figure 6C). Males did not show any alterations in PDH expression (Figures 6D and 6E), although the activity was significantly reduced in male HM group (Figure 6F). Therefore, although the expression level of PDH was similar to or higher than that in the WT group, activity was significantly reduced in both sexes, and this could be attributed to the decreased synthesis of lipoic acid reported in NFU1^{G208C} patients (20). The inhibition of PDH activity correlated with a severe attenuation of lipoic acid binding to PDH (Figures 6G–6J). Decreased lipoylation of

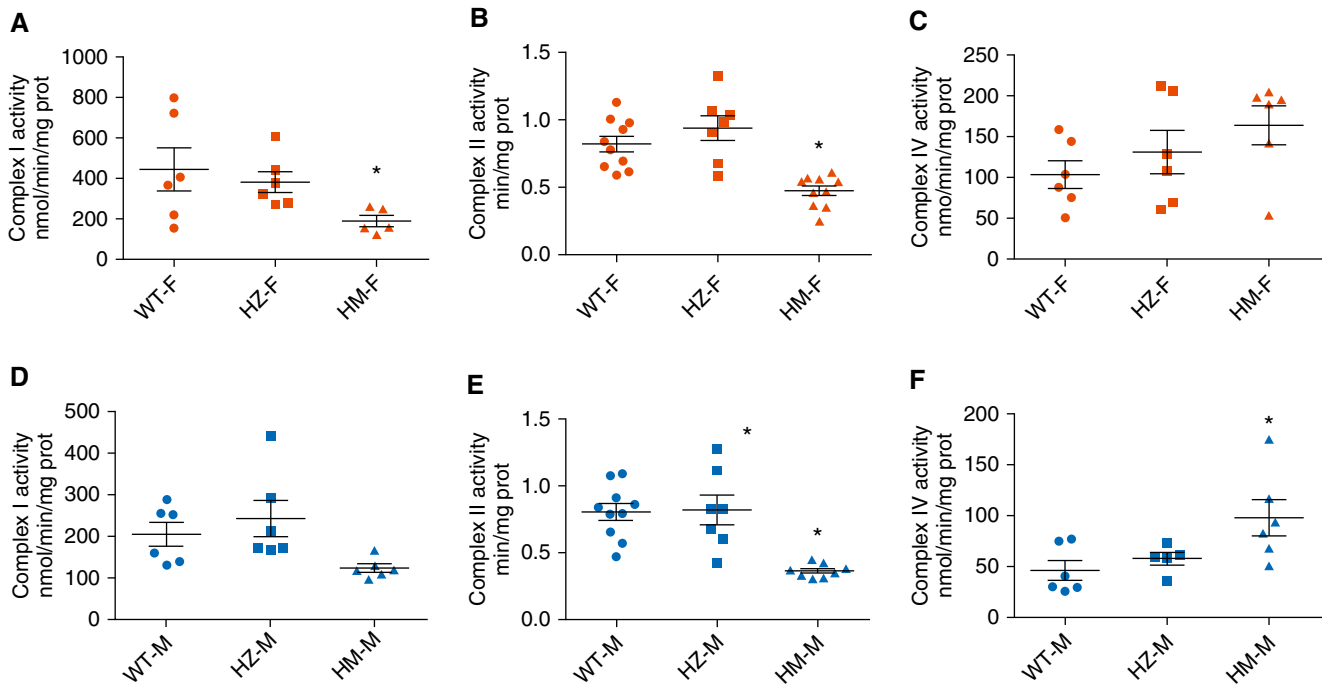


Figure 3. Alteration in the activities of electron transport chain complexes. The enzymatic activities of individual complexes were measured in mitochondria isolated from liver. (A–C) We found that in the female HM group, Complex I (A) and Complex II (B) activity was significantly decreased, whereas Complex IV activity was unchanged (C). (D–F) In males, Complex I activity was unchanged, with a downward trend in the HM group (D); Complex II activity was significantly decreased (E); and Complex IV activity was significantly elevated in the HM group (F). Data are presented as mean \pm SEM, $n = 5–10$, * $P < 0.05$ versus control, ANOVA.

PDH was also described in pulmonary artery endothelial cells, with an attenuated expression of BOLA3 (BoLA Family Member 3), another protein that is involved in the regulation of Fe-S biogenesis (32). These previously published data strongly support the importance of Fe-S homeostasis for maintaining adequate PDH activity.

Iron Regulatory Proteins

Two main scaffold proteins are involved in the biosynthesis, transport, and insertion of Fe-S clusters: NFU and ISCU. The roles of these scaffold proteins and their ability to substitute for each other or work cooperatively are still under debate. We examined whether NFU1 deficiency could affect ISCU protein levels. We found that females did not exhibit any alteration in

ISCU levels (Figures 7A and 7B); however, males in the HM group had significantly upregulated ISCU (Figures 7C and 7D). This increase in ISCU protein levels may have additionally protected males from an NFU1 deficiency. Aconitase is an important enzyme in the TCA cycle, but it can serve as a transcription factor in the event of decreased iron metabolism. Activation of aconitase-induced transcription leads to the accumulation of ferritin, an important protein that transports iron. Our examination of aconitase and ferritin levels in the lungs showed a significant accumulation of ferritin in HZ, but not HM, females (Figures 8A and 8B). Aconitase levels remained unchanged (Figure 8C). In males, there were no significant changes in either aconitase or ferritin

(Figures 8D–8F). These results indicate that NFU1 deficiency did not alter overall iron homeostasis and did not lead to ferritin and aconitase disturbances.

Discussion

In this study, we proved that the induction of mitochondrial dysfunction via genetic manipulation is sufficient to produce a PH phenotype. Abnormal function of the mitochondria is well documented in PAH; however, the causative link between mitochondrial dysfunction and PAH development has never been established. The Fe-S cluster system is important for normal mitochondrial function, but the role of this system in PAH pathogenesis

Figure 2. (Continued). versus control, ANOVA; for each animal, a random 10 vessels were averaged). (C) Representative three-dimensional micro-computed tomography images of the pulmonary vasculature in WT and HM female rats. Three different views of each lung are shown. (D) Representative microangiogram images show the vascular morphology of the right middle lobe of female WT and HM rats (scale bars: 5 mm) and the morphology of small pulmonary arteries (scale bars: 1 mm). Double-sided arrows show that HM rats have an increase in the area of low vascular density. This decrease in the complexity and number of the small pulmonary arteries could be due to a combination of pulmonary arterial hypertension-associated microvascular rarefaction and vasoobliterative disease. The arrowheads point to multiple occlusions of the small pulmonary arteries that appear as a break in pulmonary artery integrity or as an extraslim section.

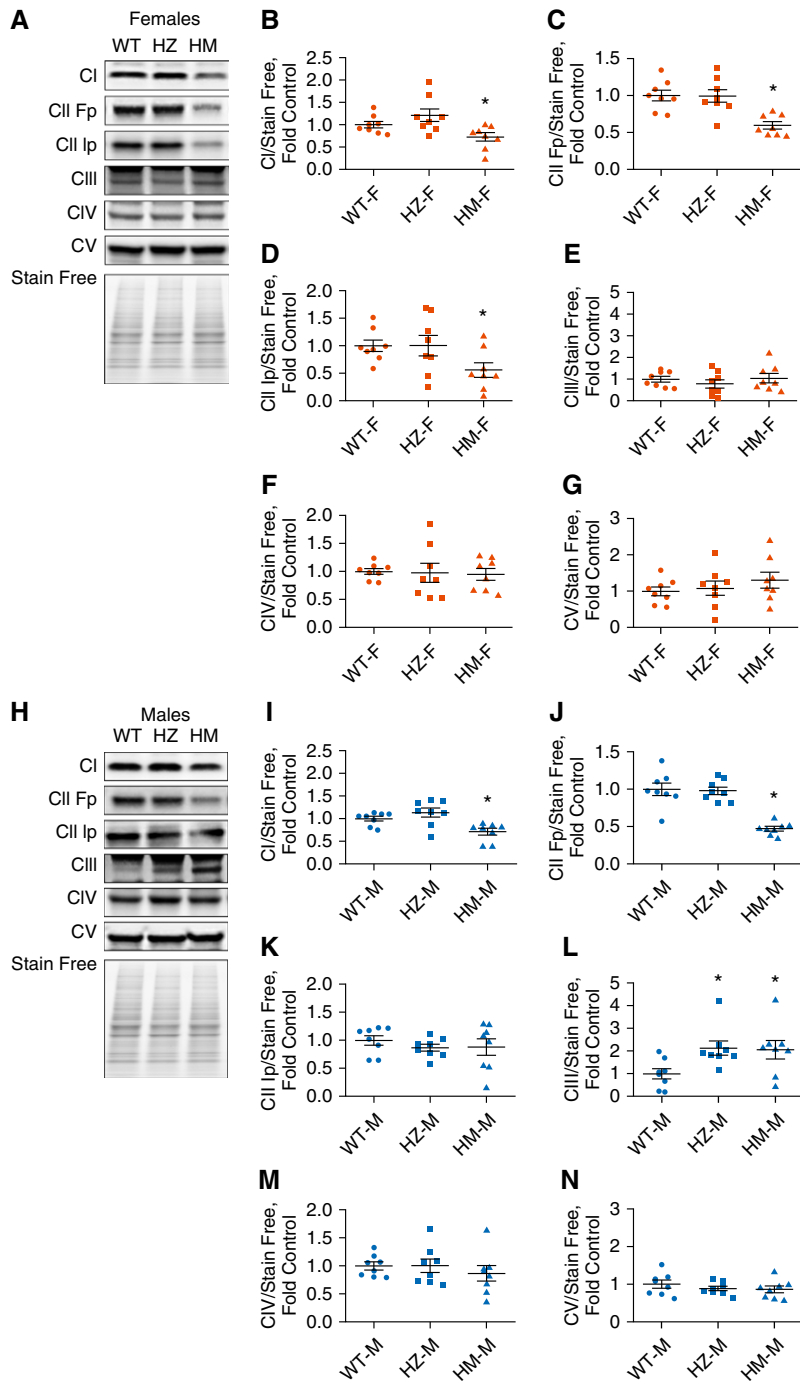


Figure 4. Expression levels of oxidative phosphorylation complexes. (A–D) Using an oxidative phosphorylation antibody cocktail, we found that in females (A), HM rats with the *NFU1* mutation showed a significant decrease in the Complex I subunit (NDUFB8) (B) and both Complex II subunits (SDHA [Fp] [C] and SDHB [Ip] [D]). (E–G) There were no changes in expression of the Complex III subunit (UQCRC2) (E), Complex IV subunit (MCTO1) (F), or Complex V subunit (ATP5A) (G). (H–J) In males (H), the HM group showed a decrease only in expression of Complex I (I) and the Complex II SDHA subunit (J). (K and L) The SDHB subunit (K) was unaltered, whereas Complex III expression was increased, in both the HZ and HM groups (L). (M and N) Complex IV (M) and Complex V (N) subunits were similar to control. Data are presented as mean \pm SEM, $n = 7–9$, * $P < 0.05$ versus control, ANOVA.

is understudied. Chan and colleagues previously reported that hypoxia-mediated repression of ISCU, an Fe-S scaffold protein, attenuates the activity of Fe-S proteins that control mitochondrial metabolism (33). Moreover, the epigenetic regulation of ISCU under PH conditions (24) leads to increased glycolysis and proliferation of the lung vasculature. In our work, we further explored the role of the *NFU1* protein, which is involved in Fe-S cluster assembly, in the pathogenesis of PAH.

The *NFU1* protein is crucial for Fe-S cluster biosynthesis and transport, and the final assembly of Fe-S-required mitochondrial enzymes. A mutation in *NFU1* results in the development of PH in 70% of clinical cases (20), whereas in the general population, this percentage is low ($\sim 0.001\%$). Mutations in the *BMPR2* (bone morphogenetic protein receptor 2) in familial PAH cases result in PAH development after 30–40 years of age (13), and the penetrance of PAH in *BMPR2* mutation carriers is only 10–20% in humans. A G208C mutation in *NFU1* results in PAH manifestation in infants before 15 months of age (20), with a penetrance of PAH of $\sim 70\%$. Using the CRISPR/Cas9 genome editing technique, we developed a point nucleotide substitution that resulted in whole-body expression of the *NFU1*^{G206C} mutant protein on the background of SD rats. These rats reproduced the *NFU1*^{G208C} mutation in humans.

Our assessment of the molecular bases for *NFU1* mutation-induced mitochondrial dysfunction in rats revealed a deficiency in Complexes I and II, and greatly reduced PDH activity. Remarkably, similar changes in Complexes I and II and PDH were previously reported in patients with *NFU1* mutations (25). Thus, our model strongly replicates the human disease. Our previous study performed in MCT rat models showed derangements in Complex I that resulted in a glycolytic switch in smooth muscle cells (1) and the lung metabolome (34). Thus, MCT- and *NFU1*-deficiency rat models share a mechanism of respiratory chain dysfunction leading to a pathological glycolytic switch in the lungs. Indeed, if efficient ATP production by oxidative phosphorylation is impaired, cells are forced to use glycolysis for their energy demands. Thus, the inhibition of electron flux via OXPHOS results in the upregulation of glycolysis, as we found in

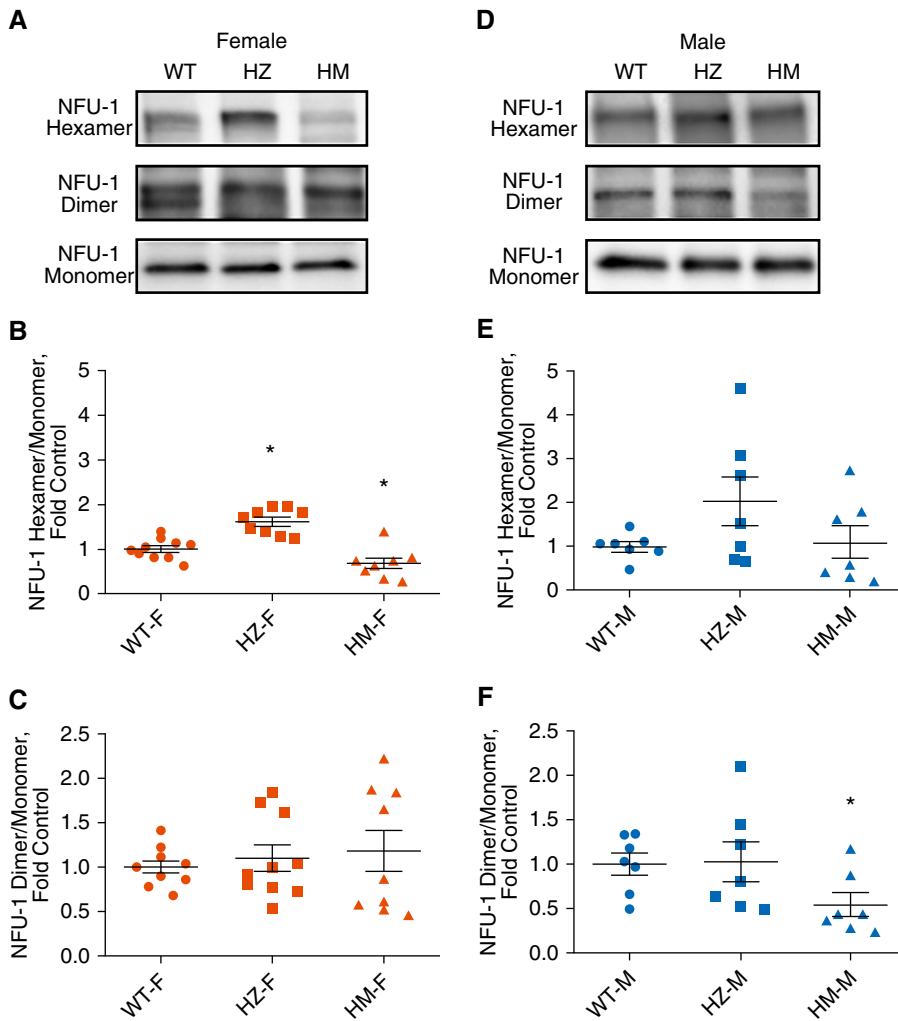


Figure 5. The oligomeric state of NFU1. (A–C) Mitochondrial separation of NFU1 oligomers on a semipreparative gel showed increased hexameric form in the HZ group and decreased hexameric form in the female HM group (A and B); a dimeric form of NFU1 was unchanged (A and C). (D–F) In males, mitochondria NFU1 oligomers showed unchanged levels of the hexameric form (D and E) and significantly reduced dimers in the HM group (D and F). Data are presented as mean \pm SEM, $n = 6-9$, * $P < 0.05$ versus control, ANOVA.

endothelial and smooth muscle cells treated with a Complex III inhibitor (16). Smooth muscle cells are also shifted from a contractile to a proliferative phenotype, and this shift is controlled by mitochondria (35). The glycolytic switch (i.e., the Warburg effect) is known to contribute to cell proliferation (36).

The PDH complex is an important component of the mitochondria that controls the entrance of pyruvate into the TCA cycle and the proper function of the OXPHOS pathway. PDH activity is tightly regulated by PDH kinase and phosphatase. PDH dysfunction was previously implicated in PAH pathogenesis (37). Inhibition of

PDH kinase by treatment with the PDH agonist dichloroacetate was shown to be protective in an animal model of PAH (38, 39), and to improve PAH in genetically susceptible patients with idiopathic PAH (10). A PDH deficiency in patients with the NFU1 mutation was previously reported (20) and occurred mainly due to decreased activity of LAS, an Fe-S-containing enzyme that forms lipoic acid, an important cofactor for PDH. Indeed, lipoylation of PDH in our model was severely impaired, which correlated with a significant drop in PDH activity. Thus, in our model, NFU1 deficiency undermines two important mitochondrial

pathways, the electron transport chain of OXPHOS and the PDH complex of the Krebs cycle, resulting in the development of PAH without any stimulation.

In this study, we confirmed that homozygous NFU1^{G208C} rats recapitulate the PAH phenotype. This includes not only impaired mitochondrial function but also changes in hemodynamic parameters. Changes in systemic blood pressure have not been previously reported for patients with an NFU1 deficiency, and we confirmed that the NFU1 mutation did not produce systemic hypertension, increased heart rates, or hypertrophic changes in the LV (Table 1). Nevertheless, this point mutation in the NFU1 gene was sufficient to initiate PH, as evidenced by the significantly elevated RVSP, RV hypertrophy, and the severe remodeling of pulmonary arteries. Interestingly, we also observed an uncoupling between RV pressure and RV remodeling, suggesting that mitochondrial dysfunction could directly stimulate the development of RV hypertrophy. Indeed, it is well recognized that mitochondria play an important role in the mechanisms responsible for cardiac hypertrophy (40). It was reported that even compensated hypertrophy was associated with decreased activity of mitochondrial respiratory complexes (41), and that the degree of mitochondrial deficiency significantly correlated with the degree of cardiac hypertrophy (42). Thus, one could expect that severely impaired mitochondrial function would additionally amplify cardiac hypertrophy in response to an increased workload. Our animal model showed a significant remodeling of small- to medium-sized pulmonary arteries, with a decrease in the cross-sectional area of the pulmonary vascular bed. This combination of elevated RV afterload and impaired mitochondrial respiration would predispose to early RV dysfunction. It was previously reported that an impairment of RV relaxation is one of the primary markers of the early RV dysfunction (43) that precedes an alteration in RV contractility and a reduction in cardiac output. Indeed, the significant decrease in the rate of pressure drop during the IRP suggests the alteration in RV relaxation that usually is attributed to increased RV stiffness due to RV hypertrophy.

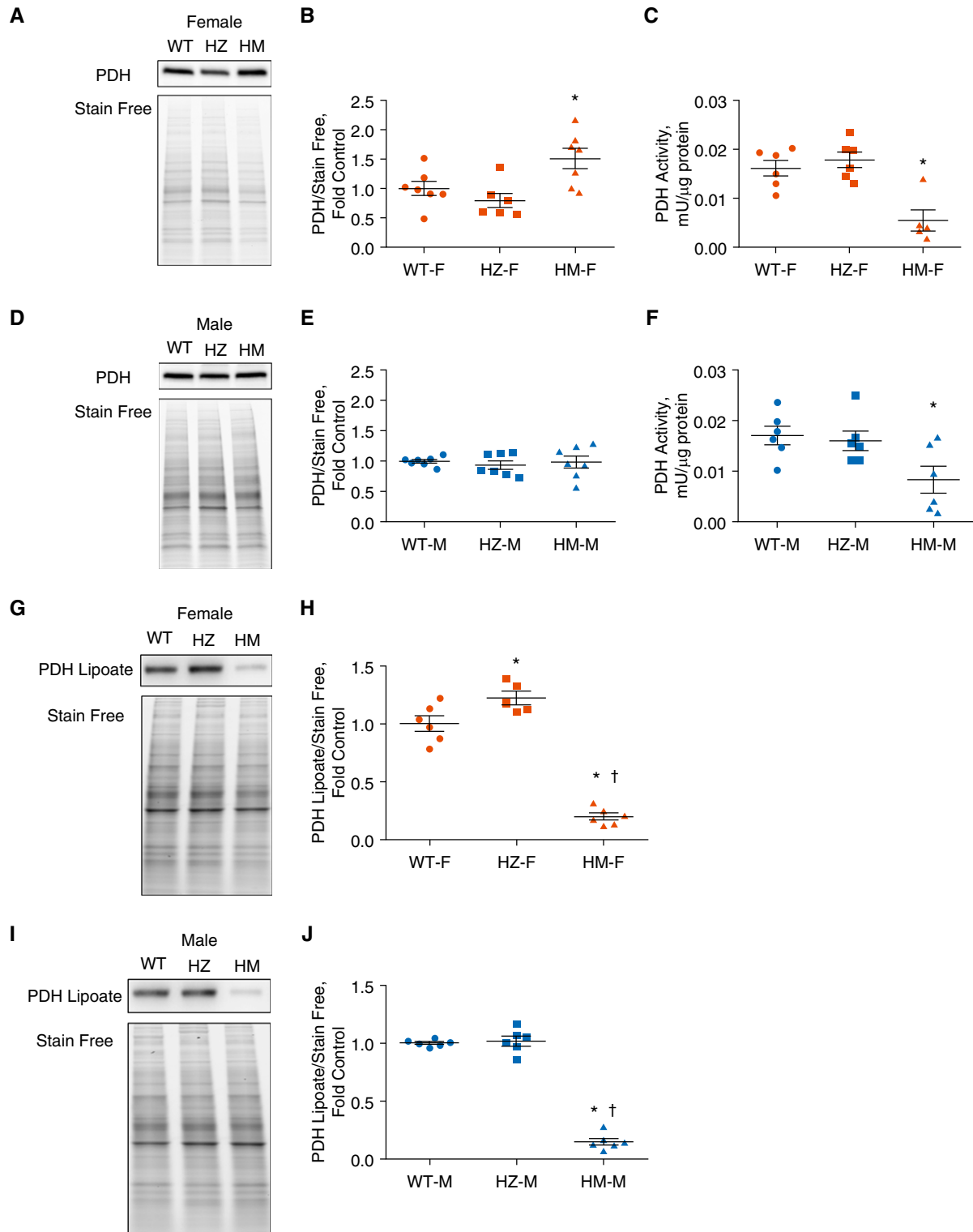


Figure 6. Pyruvate dehydrogenase (PDH) activity and expression. (A and B) Western blot showed increased expression levels of PDH in the lung lysates of female HM rats. (C) However, PDH activity in mitochondria lysate was significantly decreased. (D–F) In males, Western blot analysis showed unchanged levels of PDH expression (D and E), but activity was decreased in the HM group (F). Changes in PDH activity were strongly correlated with the level of PDH lipoylation. (G–J) In HM groups of either sex, the amount of lipoate-containing PDH was severely downregulated, confirming that a mutation in the NFU1 protein mediates impaired lipoic acid synthesis. Data are presented as mean \pm SEM, $n = 5–7$, $*P < 0.05$ versus control, ANOVA. $\dagger P < 0.05$ versus HZ.

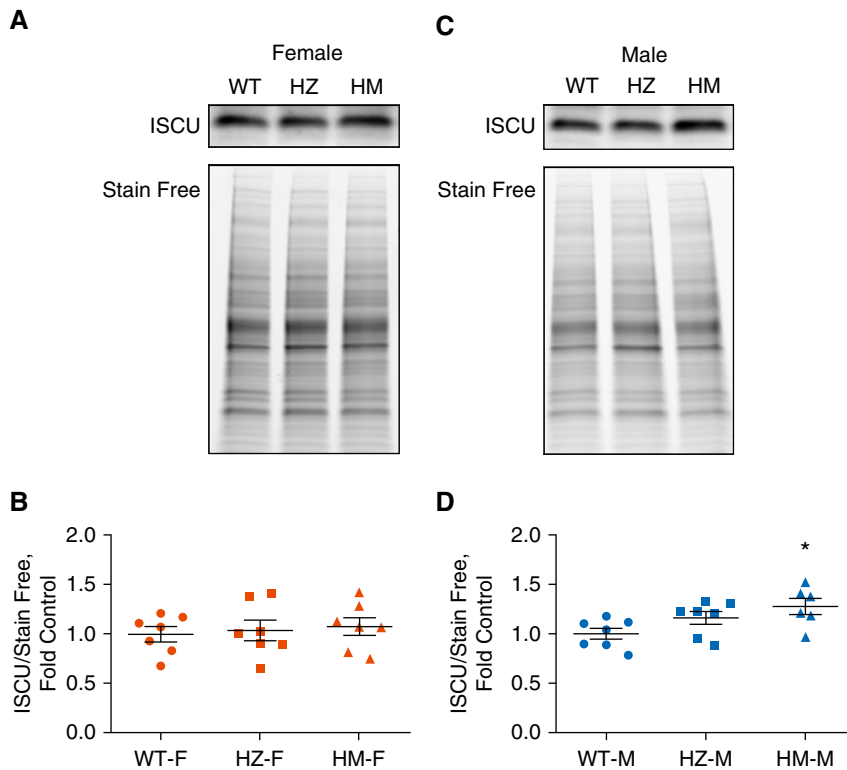


Figure 7. Iron-sulfur cluster scaffold protein ISCU. (A and B) Western blot analysis of female lung lysates (A) showed unaltered protein levels of ISCU (B). (C and D) In contrast, in males, the levels of ISCU protein were found to be significantly increased in the HM group. Data are presented as mean \pm SEM, $n = 6-7$, * $P < 0.05$ versus control, ANOVA.

Interestingly, the model also showed an uncoupling between RV pressure and the level of pulmonary vascular remodeling, as the remodeling present in the HM male group and HZ groups did not correlate with the RVSP. Given that the NFU1 mutation significantly compromises the function of the LV, as evidenced by decreased systemic blood pressure and the size of the LV (Table 1), it could be expected that the same mitochondrial dysfunction should equally affect the size and function of the RV. Therefore, the elevation of RVSP or RV/LV+S in HZ and HM male rats back to or slightly above the WT levels, contrary to RV inhibition driven by mitochondrial dysfunction, could represent a “missing” response of the RV hemodynamics to an increased afterload. Future studies to characterize the function of the RV and LV *in vivo* and *ex vivo* will help us understand the mechanisms behind the discovered discrepancies in this animal model.

The most surprising observation in the NFU1 model was the sex dimorphism in PAH development. Although we previously

reported a sex dimorphism in disease manifestation in the Sugen/hypoxia model (27) due to the predisposition of males to inflammation and females to proliferation, all of the rats developed PAH. In our new, humanized rat model, the PAH phenotype predominantly developed in HM female rats. Based on the Fulton index, females had a 67% penetrance for the PAH phenotype, whereas males had only a 20% penetrance. This gives a 3:1 sex ratio, which is similar to the sex-skewed incidence of PAH observed clinically. To our knowledge, this is the first animal model to recapitulate this sex difference in the development of PAH. Spontaneous PAH development in NFU1^{G206C} female rats may indicate the intrinsic importance of Fe-S cluster metabolism or sensitivity to altered energy production specifically in females, or it could also indicate a sex dimorphism in the adaptation. In the present study, we documented some sex-specific mechanisms that could be responsible for this sex difference. We found at least two components that could explain the reduced

PAH phenotype in males. The first is related to the plasticity of the electron transport chain to Fe-S cluster deficiency in males. Complex I activity was extensively reduced in females, but not in males. Together with increased Complex III expression and Complex IV activity, this may indicate an overall OXPHOS resistance to the main Complex II deficiency in males. Therefore, we can speculate that the electron transport chain of the male sex has additional flexibility and adaptive features. The second possible contributor to the sex dimorphism is the upregulation of the ISCU Fe-S scaffold protein in males in response to NFU1 deficiency. It was previously reported that ISCU could form a heterocomplex with NFU1 and assist with Fe-S cluster insertion into NFU1 (44). The ISCU protein may also substitute dysfunctional NFU1 for Fe-S cluster chaperon and transfer functions. Moreover, oligomerization of NFU1 could be important, as we did not observe any disturbances in hexameric NFU1 in males, but found reduced hexamers in female rats. Taken together, these observations suggest that the flexibility of the male sex in restoring balance to the OXPHOS and Fe-S cluster metabolism may play a key role in reduced PAH phenotype. Nevertheless, despite all of these protection mechanisms, the males exhibited a more pronounced RV dysfunction, which was confirmed by a male-specific increase in the RV end-diastolic pressure. This predisposition of the male sex to RV failure is well recognized in the field (27, 29) but is not fully understood. We believe that our model will help clarify the particular mechanisms that are responsible for the manifestation of PAH in both sexes.

In conclusion, we found that mitochondrial dysfunction resulting from an Fe-S system deficiency increased the risk of PH. The humanized rat model of the NFU1 mutation, which reproduces the known human polymorphism, was found to possess both PAH and MMS1 phenotypes. This model could be used to study the intrinsic mechanisms of mitochondrial dysfunction and the role of Fe-S cluster homeostasis in both diseases. This is the first genetic rat model for PAH (45) and the first animal model for MMS1. Our data also indicate that at 3 months of age, female rats had more predominant changes in heart hypertrophy than in pulmonary pressure.

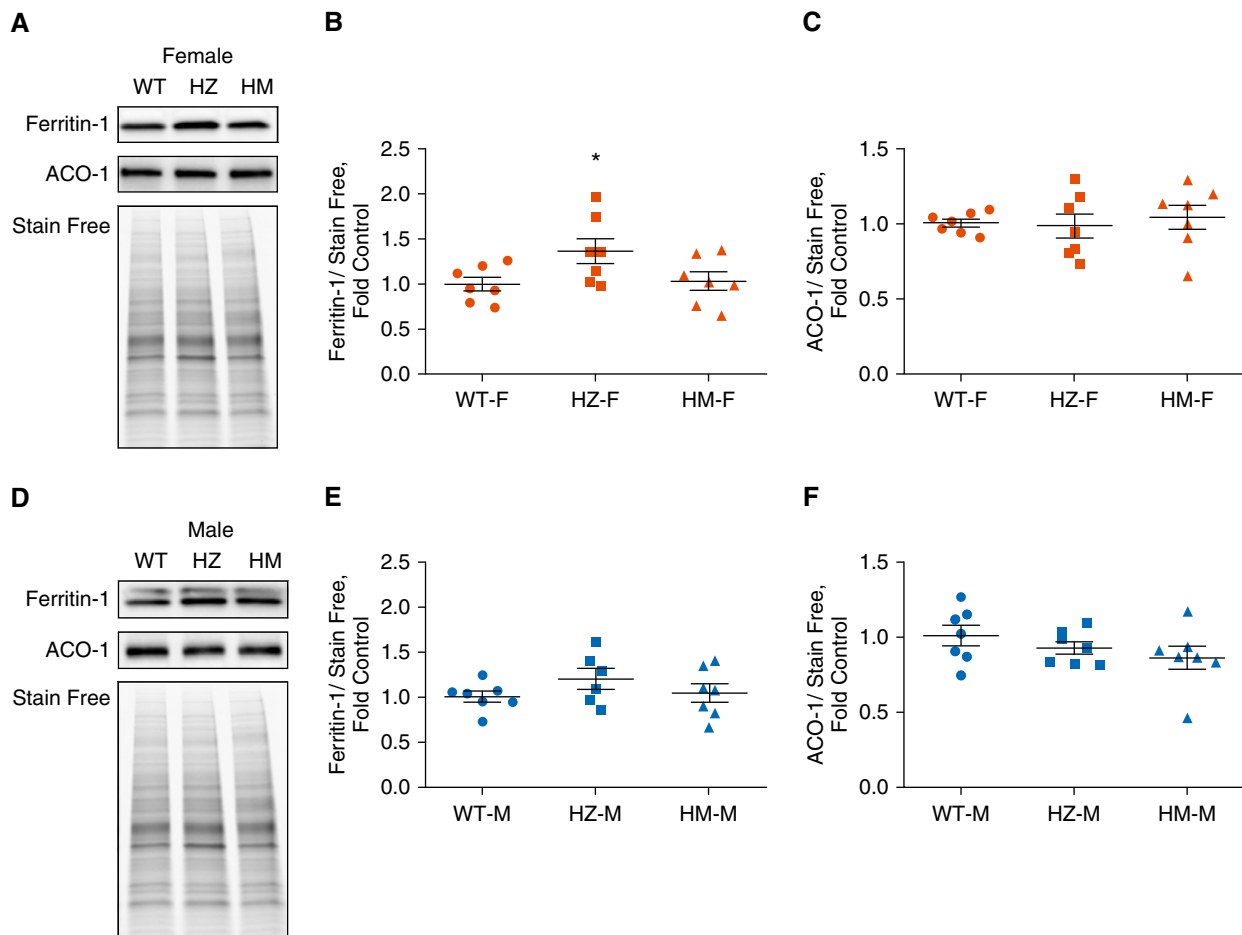


Figure 8. Aconitase (ACO) and ferritin levels in lung lysates. (A–C) Western blot analysis indicates a slight increase in ferritin levels (A and B) in the HZ female group and unchanged levels of aconitase (A and C). (D–F) In males, both ferritin (D and E) and aconitase (D and F) levels were similar to control. Data are presented as mean \pm SEM, $n=6-7$, * $P < 0.05$ versus control, ANOVA.

Therefore, the NFU1 mutation model can also be used to elucidate the mechanisms involved in right-heart hypertrophy. Further studies are needed to explore the mechanisms of vascular proliferation, heart

hypertrophy, metabolic derangements, and inflammation, as well as other mechanisms involved in PAH development and progression. This model may also lead to the discovery of treatment options for

currently lethal PAH and MMDS1 diseases. ■

Author disclosures are available with the text of this article at www.atsjournals.org.

References

- Rafikov R, Sun X, Rafikova O, Louise Meadows M, Desai AA, Khalpey Z, et al. Complex I dysfunction underlies the glycolytic switch in pulmonary hypertensive smooth muscle cells. *Redox Biol* 2015;6: 278–286.
- Archer SL, Gomberg-Maitland M, Maitland ML, Rich S, Garcia JG, Weir EK. Mitochondrial metabolism, redox signaling, and fusion: a mitochondria-ROS-HIF-1 α -Kv1.5 O₂-sensing pathway at the intersection of pulmonary hypertension and cancer. *Am J Physiol Heart Circ Physiol* 2008;294:H570–H578.
- Dromparis P, Paulin R, Sutendra G, Qi AC, Bonnet S, Michelakis ED. Uncoupling protein 2 deficiency mimics the effects of hypoxia and endoplasmic reticulum stress on mitochondria and triggers pseudohypoxic pulmonary vascular remodeling and pulmonary hypertension. *Circ Res* 2013;113:126–136.
- Stenmark KR, Tuder RM. Peroxisome proliferator-activated receptor γ and mitochondria: drivers or passengers on the road to pulmonary hypertension? *Am J Respir Cell Mol Biol* 2018;58:555–557.
- Paulin R, Dromparis P, Sutendra G, Gurtu V, Zervopoulos S, Bowers L, et al. Sirtuin 3 deficiency is associated with inhibited mitochondrial function and pulmonary arterial hypertension in rodents and humans. *Cell Metab* 2014;20:827–839.
- Ryan JJ, Marsboom G, Fang YH, Toth PT, Morrow E, Luo N, et al. PGC1 α -mediated mitofusin-2 deficiency in female rats and humans with pulmonary arterial hypertension. *Am J Respir Crit Care Med* 2013;187:865–878.
- Caruso P, Dunmore BJ, Schlosser K, Schoors S, Dos Santos C, Perez-Iratxeta C, et al. Identification of MicroRNA-124 as a major regulator of enhanced endothelial cell glycolysis in pulmonary arterial hypertension via PTBP1 (polypyrimidine tract binding protein) and pyruvate kinase M2. *Circulation* 2017;136:2451–2467.

8. Lundgrin EL, Park MM, Sharp J, Tang WH, Thomas JD, Asosingh K, *et al.* Fasting 2-deoxy-2-[18F]fluoro-D-glucose positron emission tomography to detect metabolic changes in pulmonary arterial hypertension hearts over 1 year. *Ann Am Thorac Soc* 2013;10:1–9.
9. Sun X, Kumar S, Sharma S, Aggarwal S, Lu Q, Gross C, *et al.* Endothelin-1 induces a glycolytic switch in pulmonary arterial endothelial cells via the mitochondrial translocation of endothelial nitric oxide synthase. *Am J Respir Cell Mol Biol* 2014;50:1084–1095.
10. Michelakis ED, Gurtu V, Webster L, Barnes G, Watson G, Howard L, *et al.* Inhibition of pyruvate dehydrogenase kinase improves pulmonary arterial hypertension in genetically susceptible patients. *Sci Transl Med* 2017;9:eaa04583.
11. Sun X, Sharma S, Fratz S, Kumar S, Rafikov R, Aggarwal S, *et al.* Disruption of endothelial cell mitochondrial bioenergetics in lambs with increased pulmonary blood flow. *Antioxid Redox Signal* 2013;18:1739–1752.
12. Zhuang W, Lian G, Huang B, Du A, Gong J, Xiao G, *et al.* CPT1 regulates the proliferation of pulmonary artery smooth muscle cells through the AMPK-p53-p21 pathway in pulmonary arterial hypertension. *Mol Cell Biochem* 2019;455:169–183.
13. Adesina SE, Kang BY, Biji KM, Ma J, Cheng J, Murphy TC, *et al.* Targeting mitochondrial reactive oxygen species to modulate hypoxia-induced pulmonary hypertension. *Free Radic Biol Med* 2015;87:36–47.
14. Pak O, Scheibe S, Esfandiary A, Gierhardt M, Sydykov A, Logan A, *et al.* Impact of the mitochondria-targeted antioxidant MitoQ on hypoxia-induced pulmonary hypertension. *Eur Respir J* 2018;pii:1701024.
15. Parra V, Bravo-Sagua R, Norambuena-Soto I, Hernández-Fuentes CP, Gómez-Contreras AG, Verdejo HE, *et al.* Inhibition of mitochondrial fission prevents hypoxia-induced metabolic shift and cellular proliferation of pulmonary arterial smooth muscle cells. *Biochim Biophys Acta Mol Basis Dis* 2017;1863:2891–2903.
16. Rafikova O, Srivastava A, Desai AA, Rafikov R, Tofovist SP. Recurrent inhibition of mitochondrial complex III induces chronic pulmonary vasoconstriction and glycolytic switch in the rat lung. *Respir Res* 2018;19:69.
17. Kollberg G, Tulinius M, Melberg A, Darin N, Andersen O, Holmgren D, *et al.* Clinical manifestation and a new ISCU mutation in iron-sulphur cluster deficiency myopathy. *Brain* 2009;132:2170–2179.
18. Legati A, Reyes A, Ceccatelli Berti C, Stehling O, Marchet S, Lamperti C, *et al.* A novel de novo dominant mutation in ISCU associated with mitochondrial myopathy. *J Med Genet* 2017;54:815–824.
19. Mochel F, Knight MA, Tong WH, Hernandez D, Ayyad K, Taivassalo T, *et al.* Splice mutation in the iron-sulfur cluster scaffold protein ISCU causes myopathy with exercise intolerance. *Am J Hum Genet* 2008;82:652–660.
20. Navarro-Sastre A, Tort F, Stehling O, Uzarska MA, Arranz JA, Del Toro M, *et al.* A fatal mitochondrial disease is associated with defective NFU1 function in the maturation of a subset of mitochondrial Fe-S proteins. *Am J Hum Genet* 2011;89:656–667.
21. Olsson A, Lind L, Thornell LE, Holmberg M. Myopathy with lactic acidosis is linked to chromosome 12q23.3-24.11 and caused by an intron mutation in the ISCU gene resulting in a splicing defect. *Hum Mol Genet* 2008;17:1666–1672.
22. Haack TB, Rolinski B, Haberberger B, Zimmermann F, Schum J, Strecker V, *et al.* Homozygous missense mutation in BOLA3 causes multiple mitochondrial dysfunctions syndrome in two siblings. *J Inherit Metab Dis* 2013;36:55–62.
23. Nishioka M, Inaba Y, Motobayashi M, Hara Y, Numata R, Amano Y, *et al.* An infant case of diffuse cerebrosplinal lesions and cardiomyopathy caused by a BOLA3 mutation. *Brain Dev* 2018;40:484–488.
24. White K, Lu Y, Annis S, Hale AE, Chau BN, Dahlman JE, *et al.* Genetic and hypoxic alterations of the microRNA-210-ISCU1/2 axis promote iron-sulfur deficiency and pulmonary hypertension. *EMBO Mol Med* 2015;7:695–713.
25. Ahting U, Mayr JA, Vanlander AV, Hardy SA, Santra S, Makowski C, *et al.* Clinical, biochemical, and genetic spectrum of seven patients with NFU1 deficiency. *Front Genet* 2015;6:123.
26. Rafikova O, Rafikov R, Kumar S, Sharma S, Aggarwal S, Schneider F, *et al.* Bosentan inhibits oxidative and nitrosative stress and rescues occlusive pulmonary hypertension. *Free Radic Biol Med* 2013;56:28–43.
27. Rafikova O, Rafikov R, Meadows ML, Kangath A, Jonigk D, Black SM. The sexual dimorphism associated with pulmonary hypertension corresponds to a fibrotic phenotype. *Pulm Circ* 2015;5:184–197.
28. Leeuwenburgh BP, Steendijk P, Helbing WA, Baan J. Indexes of diastolic RV function: load dependence and changes after chronic RV pressure overload in lambs. *Am J Physiol Heart Circ Physiol* 2002;282:H1350–H1358.
29. Escribano-Subias P, Blanco I, López-Meseguer M, Lopez-Guarch CJ, Roman A, Morales P, *et al.*; REHAP investigators. Survival in pulmonary hypertension in Spain: insights from the Spanish registry. *Eur Respir J* 2012;40:596–603.
30. Cai K, Liu G, Frederick RO, Xiao R, Montelione GT, Markley JL. Structural/functional properties of human NFU1, an intermediate [4Fe-4S] carrier in human mitochondrial iron-sulfur cluster biogenesis. *Structure* 2016;24:2080–2091.
31. Sutendra G, Dromparis P, Bonnet S, Haromy A, McMurtry MS, Bleackley RC, *et al.* Pyruvate dehydrogenase inhibition by the inflammatory cytokine TNF α contributes to the pathogenesis of pulmonary arterial hypertension. *J Mol Med (Berl)* 2011;89:771–783.
32. Yu Q, Tai YY, Tang Y, Zhao J, Negi V, Culley MK, *et al.* BOLA (BoLA Family Member 3) deficiency controls endothelial metabolism and glycine homeostasis in pulmonary hypertension. *Circulation* 2019;139:2238–2255.
33. Chan SY, Zhang YY, Hemann C, Mahoney CE, Zweier JL, Loscalzo J. MicroRNA-210 controls mitochondrial metabolism during hypoxia by repressing the iron-sulfur cluster assembly proteins ISCU1/2. *Cell Metab* 2009;10:273–284.
34. Rafikova O, Meadows ML, Kinchen JM, Mohny RP, Maltepe E, Desai AA, *et al.* Metabolic changes precede the development of pulmonary hypertension in the monocrotaline exposed rat lung. *PLoS One* 2016;11:e0150480.
35. Chiong M, Cartes-Saavedra B, Norambuena-Soto I, Mondaca-Ruff D, Morales PE, García-Miguel M, *et al.* Mitochondrial metabolism and the control of vascular smooth muscle cell proliferation. *Front Cell Dev Biol* 2014;2:72.
36. Vander Heiden MG, Cantley LC, Thompson CB. Understanding the Warburg effect: the metabolic requirements of cell proliferation. *Science* 2009;324:1029–1033.
37. Ryan JJ, Archer SL. Emerging concepts in the molecular basis of pulmonary arterial hypertension: part I: metabolic plasticity and mitochondrial dynamics in the pulmonary circulation and right ventricle in pulmonary arterial hypertension. *Circulation* 2015;131:1691–1702.
38. Li B, Yan J, Shen Y, Liu Y, Ma Z. Dichloroacetate prevents but not reverses the formation of neointimal lesions in a rat model of severe pulmonary arterial hypertension. *Mol Med Rep* 2014;10:2144–2152.
39. McMurtry MS, Bonnet S, Wu X, Dyck JR, Haromy A, Hashimoto K, *et al.* Dichloroacetate prevents and reverses pulmonary hypertension by inducing pulmonary artery smooth muscle cell apoptosis. *Circ Res* 2004;95:830–840.
40. Facundo HDTF, Brainard RE, Caldas FRL, Lucas AMB. Mitochondria and cardiac hypertrophy. *Adv Exp Med Biol* 2017;982:203–226.
41. Griffiths ER, Friehs I, Scherr E, Poutias D, McGowan FX, Del Nido PJ. Electron transport chain dysfunction in neonatal pressure-overload hypertrophy precedes cardiomyocyte apoptosis independent of oxidative stress. *J Thorac Cardiovasc Surg* 2010;139:1609–1617.
42. Lin CS, Sun YL, Liu CY. Structural and biochemical evidence of mitochondrial depletion in pigs with hypertrophic cardiomyopathy. *Res Vet Sci* 2003;74:219–226.
43. Murch SD, La Gerche A, Roberts TJ, Prior DL, MacIsaac AI, Burns AT. Abnormal right ventricular relaxation in pulmonary hypertension. *Pulm Circ* 2015;5:370–375.
44. Wachnowsky C, Wesley NA, Fidai I, Cowan JA. Understanding the molecular basis of multiple mitochondrial dysfunctions syndrome 1 (MMDS1)—impact of a disease-causing Gly208Cys substitution on structure and activity of NFU1 in the Fe/S cluster biosynthetic pathway. *J Mol Biol* 2017;429:790–807.
45. Colvin KL, Yeager ME. Animal models of pulmonary hypertension: matching disease mechanisms to etiology of the human disease. *J Pulm Respir Med* 2014;4:198.